Asia-Pacific Journal of Atmospheric Sciences (2021) 57:347–359
https://doi.org/10.1007/s13143-020-00197-z

Online ISSN 1976-7951
Print ISSN 1976-7633

ORIGINAL ARTICLE

A Comparative Analysis of the Bay of Bengal Ocean State Using Standalone and Coupled Numerical Models

T. S Anandh[1,2] · Bijan Kumar Das[1,3] · J. Kuttippurath[1] · Arun Chakraborty[1]

Received: 6 November 2019 / Revised: 11 March 2020 / Accepted: 20 March 2020 / Published online: 23 April 2020

Abstract

This study evaluates the impact of coupled model in simulating the ocean state conditions of Bay of Bengal by comparing standalone and coupled numerical model simulations. The oceanic model is the Regional Ocean Modelling System (ROMS) and the coupled model comprises of ROMS and Weather Research and Forecast modelling system to simulate the oceanic and atmospheric state of the bay. The coupled model is initialized with atmospheric data from Global Data Assimilation System and oceanic data from Estimating the Circulation and Climate of the Ocean (ECCO). The standalone model is initiated with ECCO data and forced by European Centre for Medium Range Weather Forecasts. The simulations are set with a resolution of 12 km in the ocean and 15 km in the atmosphere for the period 2008–2014, and are compared to reanalysis and measurements. The models are compared for their ability to simulate the sea surface temperature, sea surface salinity, sea level, heat flux, sea level pressure and currents in BOB. With the exchange of atmospheric fluxes and sea surface temperature, the coupled model better captured ocean state representations than the standalone model and, matches well with that of the observations. The simulated temperature shows a warm bias in both simulations at 100–150 m depth. The models are able to simulate the seasonal reversal of boundary currents and associated eddies, and variations in heat fluxes over the ocean. The coupled model provides a better simulation of the ocean state and air–sea interaction which can further be used for climate studies over the bay.

Keywords Coupled model · ROMS · WRF · Bay of Bengal Modelling

1 Introduction

Upper ocean and the lower atmosphere are the most dynamical parts of the earth. The weather and climate over any part of the earth is determined by the air–sea interactions occurring at the atmospheric boundary layer and mixed layer of the ocean (Elsberry and Garwood Jr 1978). These interactions determine the large scale phenomenon such as El–Nino (Trenberth 1997) and monsoons (Goswami et al. 1999) as well as small scale events such as cyclones and thunderstorms (Elsberry and Garwood Jr 1978). Therefore, understanding the air–sea interactions help to determine, simulate and predict the meteorological events occurring over any region.

The Bay of Bengal (BOB or the bay) region of the Indian Ocean is enclosed by Asian landmass in the northern, eastern and western sides and by open waters in the southern side. The BOB waters remain warm (about 28 °C) for most part of the year as there is no heat exchange with polar waters (Vinayachandran and Shetye 1991). The high SST and winds during pre– and post–monsoon seasons over the bay also lead to maximum air–sea interactions that help the formation and development of cyclones frequently during these seasons (Girishkumar and Ravichandran 2012). In BOB, the large freshwater influx at the north (Subramanian 1993), high precipitation over evaporation (Prasad 1997) and stratified upper oceans (Jana et al. 2015) help to retain the warm stratified surface waters for a long time. This stratified warm surface waters further enhances the air–sea interactions. The above

Responsible Editor: Ashok Karumuri.

Electronic supplementary material The online version of this article (https://doi.org/10.1007/s13143-020-00197-z) contains supplementary material, which is available to authorized users.

✉ T. S Anandh
anandh.ts@tropmet.res.in

[1] Centre for Oceans, Rivers, Atmosphere and Land Sciences, Indian Institute of Technology Kharagpur, Kharagpur, India

[2] Indian Institute of Tropical Meteorology, Pune, India

[3] Department of Mathematics, Midnapore College (Autonomous), Midnapore, India

interactions over the BOB play a major role in determining weather of the Indian subcontinent.

The ocean state conditions over BOB are extensively studied using ship drift data (Cutler and Swallow 1984), satellite measurements (Legeckis 1987) and numerical models (Sil and Chakraborty 2011b; Chakraborty and Gangopadhyay 2016a, 2016b). The seasonal reversal of western boundary current (WBC) of the bay has been widely discussed (Babu 1992; Das et al. 2019; Shetye et al. 1990; Suryanarayana et al. 1992; Sil and Chakraborty 2011a) to analyze the influence of WBC on Indian climate. Also, the circulation in the bay are forced by the seasonal reversal of monsoon winds and remote forcings from the equator (Kumar et al. 2010; Sil and Chakraborty 2011b). However, detailed studies over BOB are limited by the availability of data. The existing satellite data are restricted to the ocean surface and insitu data are limited to the sparsity of buoys deployed in the bay. Cutler and Swallow (1984) identified the reversal of surface currents influenced by wind stress using ship drift data. Satellite data are used to identify the cyclonic and anti–cyclonic eddies associated with WBC (Dandapat and Chakraborty 2016) and to study the equatorial remote forcings on the BOB circulations (Rao et al. 2010). Various oceanic phenomena, mainly different air–sea interactions, need high resolution spatial and temporal data to better understand them. Many ocean models have been developed to tackle the problem of non–availability of high resolution data. The ocean models proposed previously for the BOB region use climatology and/or a coarser resolution atmospheric data and, henceforth, they are not adequate enough to capture different oceanic features (Sil et al. 2011; Sivareddy et al. 2015; Srivastava et al. 2016). Furthermore, data are also taken from global models to understand the air–sea interactions, through surface fluxes, to improve the prediction and assess the cyclone formations over the region. Many products such as Objectively Analyzed Flux (OAFlux), Comprehensive Ocean Atmosphere Data Set (COADS) and ERA–Interim, National Centers for Environmental Prediction (NCEP) provide these fluxes over the region. However, it has to be noted that, COADS (da Silva et al. 1994) data does not represent coastal data well. The NCEP data (Kalnay et al. 1996) have an underestimation in flux estimates in some seasons (monsoon) over the BOB region. Unavailability of continuous and a single data source for all fluxes make problem in using satellite data in analysis.

Coupled models, where the atmosphere evolves together with oceanic fields, could provide better results than using static atmospheric data. Henceforth, in this study, we compare a high resolution coupled model inter-annual simulations with that of a standalone simulations of the ocean state conditions of BOB for the period 2010–2014. Rest of the article is arranged as: section 2 includes the description of model, data and methodology used in the study, results and discussions are given in section 3 and a conclusion is written in section 4.

2 Model, Data and Methodology

2.1 The Coupled Model

The Coupled Ocean Atmosphere Wave Sediment Transport system (COAWST) model developed by Warner et al. 2010, is set up for interannual studies for BOB. The coupled model includes Regional Ocean Modelling System (ROMS) and Weather Research and Forecasting (WRF) modelling system to estimate the ocean and atmospheric state of the bay, respectively. ROMS (Haidvogel et al. 2008; Shchepetkin and McWilliams 2005), is a high resolution stretched terrain–following hydrostatic model, which solves the momentum and other primitive equations using split–explicit time–stepping schemes. Along the horizontal, the model solves the primitive equations on a staggered Arakawa C–grid. Coastal boundaries are included as a finite–discretized grid through a sea/land mask. WRF (Skamarock et al. 2008) is a fully compressible non–hydrostatic model that solves the primitive equations over a terrain following hydrostatic pressure coordinates and also uses the staggered Arakawa C–grid. Various time integration and advection schemes are used in this model to simulate the atmospheric variables.

The model simulations are customised for the BOB region at 78°E – 100°E and 4°N – 24°N. The ocean model is configured with 12 km horizontal resolution and 32 sigma vertical levels. The atmospheric model is configured with 15 km horizontal resolution and 40 vertical levels. The bottom of ocean domain is taken from the Etopo2 bathymetry data. Figure 1 shows the study domain with its bathymetry. The top of the atmospheric domain is 50 mb pressure level. The simulation is initiated on 1 January 2008 and run through the end of 2014. For the oceanic model, data from Estimating the Circulation and Climate of the Ocean version 2 (ECCO2) (Menemenlis

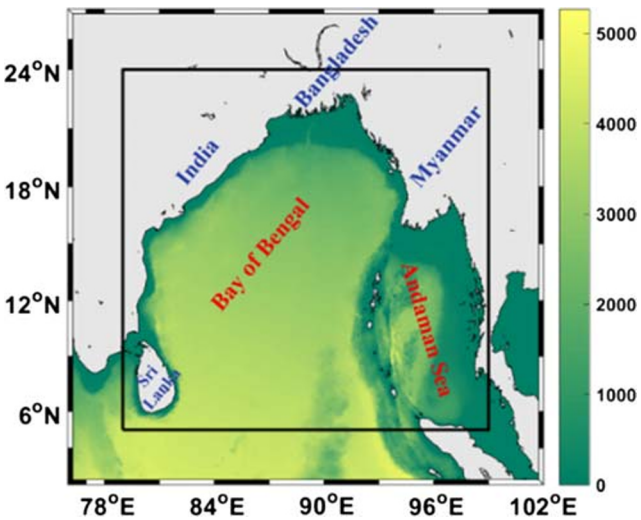

Fig. 1 The study domain, Bay of Bengal (black box) with bathymetry (shaded) from ETOPO2

et al. 2005, 2008) data, which has a temporal resolution of 3 days, are used. These data provide temperature, salinity, ocean currents and sea level for initial and lateral boundary conditions. The atmospheric data for initial and boundary conditions are taken from NCEP FNL (Final) Operational Global Analysis data for the complete simulation period. The NCEP FNL data provide necessary parameters for initialising and running the WRF model that include potential temperature, pressure, wind components, heat fluxes, mixing ratios of water, rain, ice and snow, and surface skin temperature. These data have a temporal resolution of 6 h. The atmospheric forcing needed for the standalone model is provided from European Centre for Medium Range Weather Forecasts (ECMWF) (Dee et al. 2011) reanalysis dataset with a temporal resolution of one day.

During the coupling process, the atmospheric model provides the zonal and meridional wind stress components, radiation, evaporation and precipitation data to the ocean model. The oceanic model receives the atmospheric model input for every 3 h and computes the surface fluxes of momentum, sensible heat, and latent heat using the COARE (Coupled Ocean–Atmosphere Response Experiment) algorithm (Fairall et al. 2003). The ocean model provides the Sea Surface Temperature (SST) to the atmospheric model for its simulations. Since both models have different horizontal resolution, a weighted average intermediary grid is created over each grid to interpolate and transfer the data correctly.

2.2 Data Used for Evaluation

The reanalysis datasets, Simple Ocean Data Assimilation (SODA3.3) (Carton et al. 2018), ECMWF – Ocean Re–Analysis System 4 (ECMWF–ORAS4) (Balmaseda et al. 2013), NCEP Global Ocean Data Assimilation System (NCEP–GODAS) (Saha et al. 2012), and World Ocean Database (Boyer et al. 2013), are used for the evaluation of model simulations. Satellite derived data used for evaluation include TRMM TMI (Wentz et al. 2015), AVISO TOPEX (Ducet et al. 2000), Ocean Surface Currents Analyses Real–time (OSCAR) (Bonjean and Lagerloef 2002), the Modern Era Retrospective–analysis for Research and Applications (MERRA) created from Goddard Earth Observing System Data Assimilation System Version 5 (GEOS–5) (Rienecker et al. 2011) and Advanced Scatterometer (ASCAT) mean surface winds (Bentamy and Fillon 2012). The insitu data from Array for Real–time Geostrophic Oceanography (ARGO) through the IPRC Argo Dataset (Lebedev et al. 2010) are also used for model comparison. The temperature and salinity measurements are taken from Research Moored Array for African-Asian-Australian Monsoon Analysis and Prediction (RAMA) buoys (McPhaden et al. 2009) installed at 12°N 90°E and 15°N 90°E and are also used for model mean evaluation (provided in the supplementary file).

2.3 Methodology

The simulations are carried out for 7 years (2008–2014) to include different Indian Ocean Dipole (IOD) and ENSO events. The simulations are started using ocean warm initial conditions from ECCO data. The volume averaged kinetic energy computed from the coupled model indicates that the model has reached its equilibrium state after two years. The two years (2008–2009) are taken as the spin up period and the next five years (2010–2014) simulations are used for the comparisons. The model comparison includes statistical and spatio-temporal analysis of various ocean-atmospheric parameters like, Temperature, Salinity, Sea Surface Height (SSH), Sea Level Pressure (SLP), heat fluxes, Ocean Heat Content (OHC), geopotential height and wind. The bias is calculated from the difference between model results and data, where positive values indicate higher values in model simulations. The correlation, root mean square difference and standard deviation are analysed with Taylor diagram (Taylor 2001) between different datasets and model simulations. Taylor diagram brings these statistical tools together to understand the predictability of the model.

3 Results and Discussion

The Taylor diagram for various parameters indicating the overall model performance compared to different datasets together are shown in Fig. 2. The monthly mean time series from 2010 to 2014 is used for the Taylor diagram analysis. The comparison of oceanic parameters include standalone and coupled model performances while the atmospheric parameters are compared with coupled model results alone. The Taylor diagram shows that, in most of the case, the ocean state simulated using coupled model has higher correlation with observational data than standalone model simulations. Also, the standard deviations from the observational data are smaller for coupled model simulations. Further, each of the parameters shown in the Tailor diagram is analyzed individually in the following subsections.

3.1 Surface and Subsurface Temperature

SST is one of the main parameter for evaluating a model performance. Figure 3 compares the time series of monthly mean SST with that of available datasets of SODA, WOD and TRMM TMI. Both the models capture the signature of semi–annual pattern of SST (two highs and two lows) in the bay. Figure 2a indicates the model performance in simulating SST and it shows that the coupled.

model is able to simulate the SST similar to TRMM data than other available datasets. The RMSD between the coupled model simulated SST and TRMM data is less

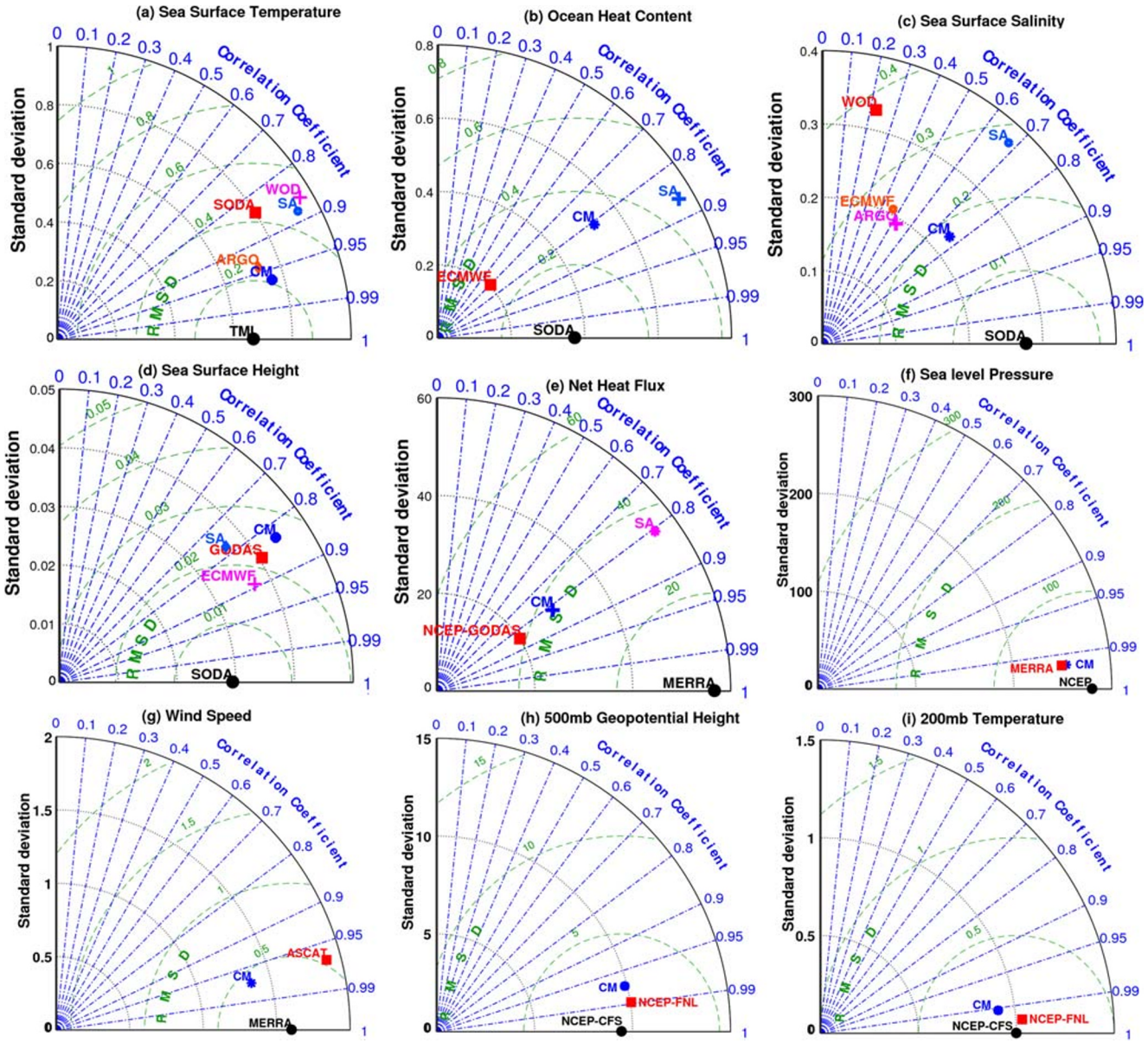

Fig. 2 Taylor Diagrams to assess the Correlation, Root Mean Square Error and standard deviation of stand-alone model (SA) and coupled model (CM) with other available datasets for (**a**) Sea Surface Temperature, (**b**) Ocean Heat Content, (**c**) Sea Surface Salinity, (**d**) Sea Surface height, (**e**) Net Heat flux, (**f**) Sea level Pressure, (**g**) Wind Speed, (**h**) 500 mb Geopotential height and, (**i**) 200 mb Temperature

than 0.2 °C, while that of standalone model is 0.45 °C and the standard deviation is about 0.8 °C throughout the simulation period. Figure 4 shows the spatial correlation and bias of SST between model and reanalysis data for the whole simulation period for standalone and coupled model, respectively. The overall correlation between TRMM data and coupled simulations is 0.96 while with that of standalone model is 0.88. The SST derived from coupled model has a correlation of 0.84 with SODA data and 0.77 with WOD data. The standalone model derived SST has a slightly better correlation of 0.86 with SODA data and 0.79 with WOD data. Furthermore, from Fig. 4, the coupled model has a warm bias at the south–eastern bay up to 0.5 °C for the simulation period, while the standalone model has more than 0.5 °C bias in these regions. The standalone model simulations have smaller warm bias and more cold bias when compared to the coupled model simulation. The standalone model simulations have very good SST correlations along the northern bay but the correlations is poor along the southern bay. The coupled model simulations have slightly smaller correlation values along the northern and central bay, although they have improved significantly along the southern bay. The simulated results from the coupled model matches well with both data, but are better compared to that of TRMM TMI. The percentage of grids showing

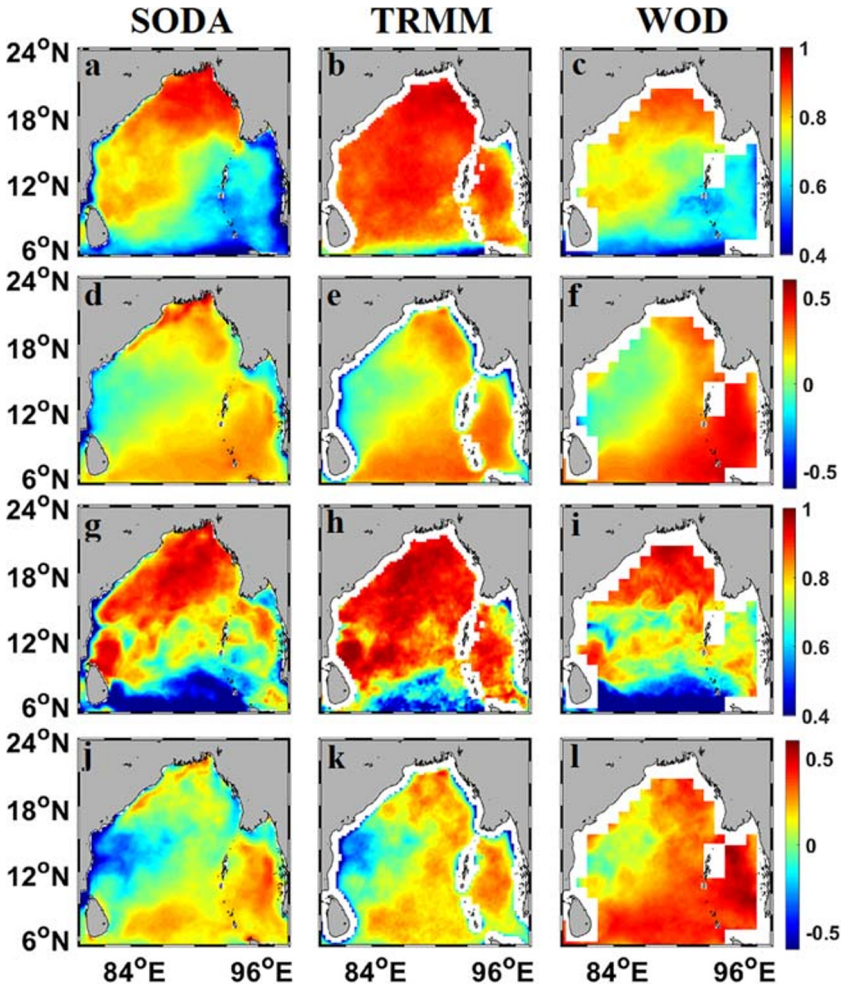

Fig. 3 The domain averaged monthly mean Sea Surface Temperature from Standalone model (SA), Coupled Model (CM), TRMM TMI, SOD and WOD

similar correlations are analysed in Supplementary S1. In Fig. 2b, the model derived ocean heat content (OHC) is compared with that from SODA and ECMWF. The model derived OHCs show a good correlation with SODA data (correlation of 0.8).

The vertical profile of temperature for the years 2010–2014 is analysed broadly to evaluate the predictive capability of the model up to 300 m, which is the most dynamic part of the oceans. Figure 5 shows the mean vertical temperature profile of the bay from the model, ECMWF and SODA. The upper ocean temperature from RAMA buoys over the bay are compared with that from the model simulations and is illustrated in Fig. S2 and S3. The standard deviation captured by the models in all vertical levels compares well with that from the reanalysis datasets. The RMSE between reanalysis data and model simulations reveal that the maximum bias occurs at 100–150 m deep whereas the agreement is very good at the surface and deep ocean. Correlation between these data also shows that the models are able to capture the surface and subsurface temperature features very well.

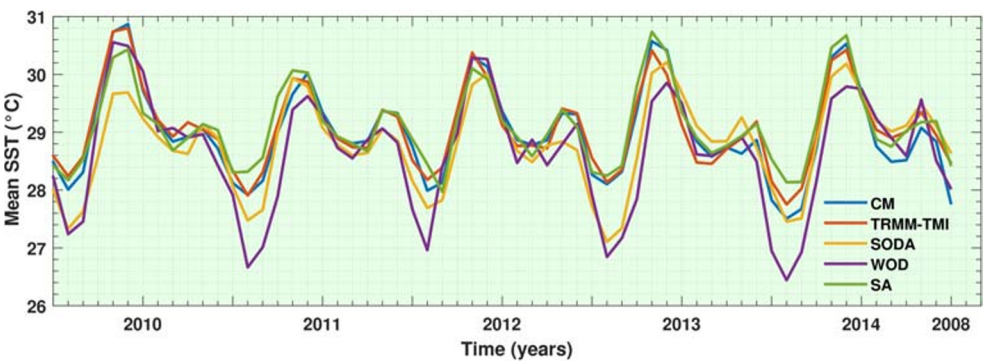

Fig. 4 Spatial Correlation (1st and 3rd row) and mean bias (2nd and 4th row) between the models and SODA, TRMM-TMI and WOD data for the period 2010–2014 SST. Top two rows represent Coupled model and bottom two rows represent standalone model

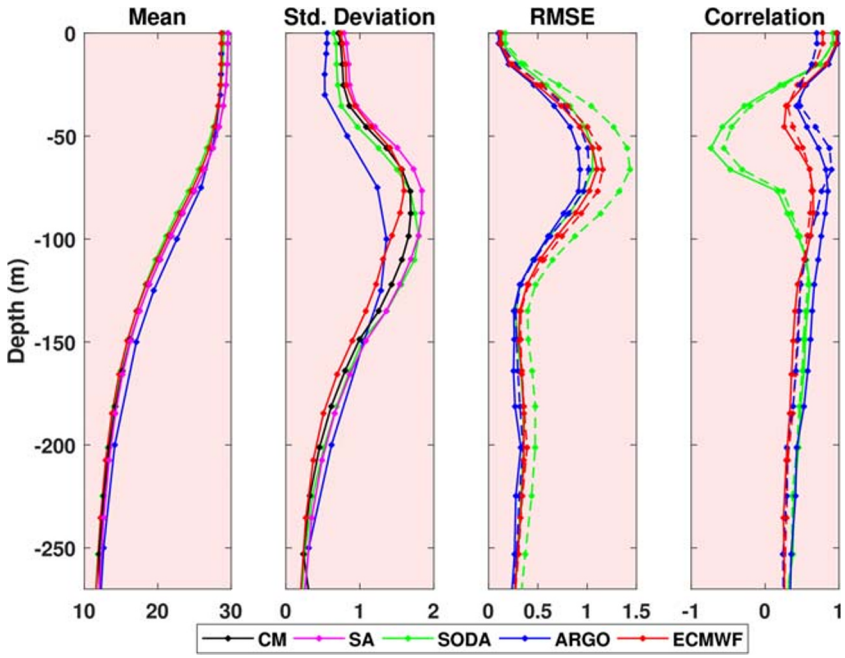

Fig. 5 Vertical profiles of temperature up to 270 m for the years 2010–2014 are compared for their mean and standard deviation with SODA, gridded ARGO and ECMWF. RMSE and Correlation are analysed between model results and each data. For RMSE and correlation, straight line shows with respect to coupled model while dotted line shows represent standalone model

3.2 Surface and Subsurface Salinity

The Sea Surface Salinity (SSS) is verified by comparing the spatial average of monthly SSS over the bay from the models, SODA and ECMWF data in Fig. 6. The comparison indicates that the simulated results are in good agreement with SODA data with a monthly mean normal bias of 0.25 psu. The salinity data after 2010 compares well with the simulated surface salinity. In Fig. 7, we analyse the spatial correlation and mean bias between the coupled and standalone simulations, and SODA and ECMWF data for the period 2010–2014, respectively. The bias in the models are apparent in the north and north eastern coastal bay where the model simulates high salinity as compared to the reanalysis data. This bias along the northern bay can be attributed to the non-inclusion of river discharge into the models. The coupled model shows better correlation and lesser bias when compared with the standalone model results. In the central bay, the bias is very small (~ <0.25 psu) and at the southern bay, the coupled model simulations show slight negative bias when compared to SODA and ECMWF data. Spatial correlation analysis between model results and reanalysis data shows that the SSS along the northern bay has very high correlation. In the Taylor diagram (Fig. 2c), the existing reanalysis and observations do not agree among themselves for the surface salinity. Furthermore, the coupled model simulated salinity matches reasonably well with SODA data in comparison with other data and standalone model results. The vertical profile analysis over the bay, in Fig. 8, indicates the models are able to reproduce the surface and subsurface salinity features well. In the top 20 m, the models show smaller standard deviation when compared to other data mainly because of the reduction in freshwater input to top layers. Small RMSE and high correlation in the subsurface layers indicate that the models well simulate the subsurface dynamics. The upper ocean salinity from RAMA buoys over the bay is compared to those from the simulations and is illustrated in Fig. S4 and S5.

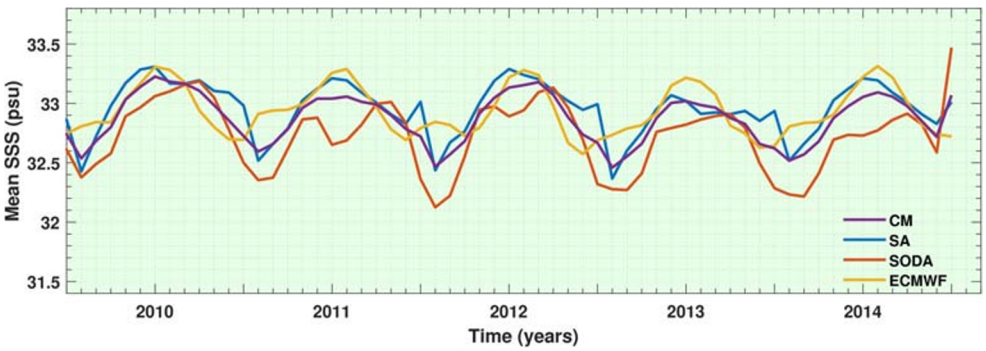

Fig. 6 The domain averaged monthly Sea Surface Salinity from model, SODA and ECMWF

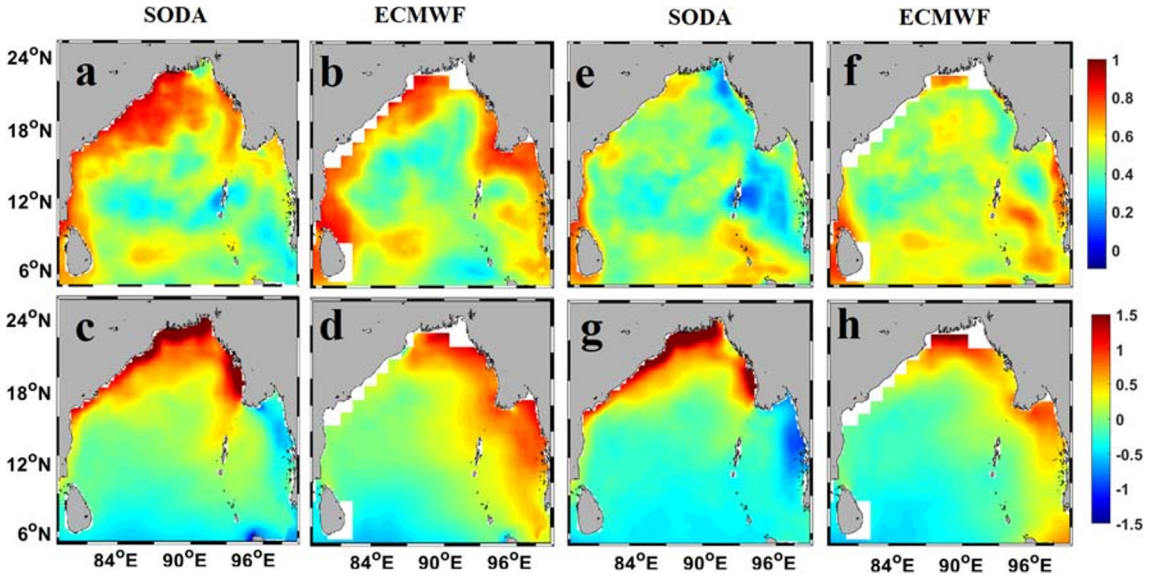

Fig. 7 Spatial Correlation (Top Row) and mean bias (Bottom Row) between the models and SODA, and ECMWF data for the period 2010–2014 sea surface salinity. Subplots a–d represents coupled model and e–h represents standalone model

3.3 Sea Surface Height

The simulated Sea Surface Height (SSH) is evaluated with AVISO–TOPEX combined data for the movement of upwelling and downwelling Kelvin waves (Rao et al. 2010) in the BOB during the year 2011. In Fig. 2d, analysis show that the coupled model simulated SSH has an overall correlation of 0.81 with SODA data with less RMSD and standard deviation of other available datasets for the period 2010–2014. The standalone model simulated SSH has smaller correlation (0.78) when compared with SODA data. Figure 9 shows SSH from the models and AVISO–TOPEX for the kelvin wave propagation over the bay. Note that upwelling creates a negative SSH while downwelling creates a positive SSH anomaly. In March, spatial pattern indicates that there exists a strong upwelling Kelvin wave (1st upwelling mode) moving along the north–eastern coast. This is followed by the downwelling Kelvin wave (1st downwelling mode) in the month of July along the same north–eastern bay. The weaker upwelling phase (2nd upwelling mode) is to be present along the south–east bay, but it is absent for the year 2011 in both TOPEX data and coupled model results. The next

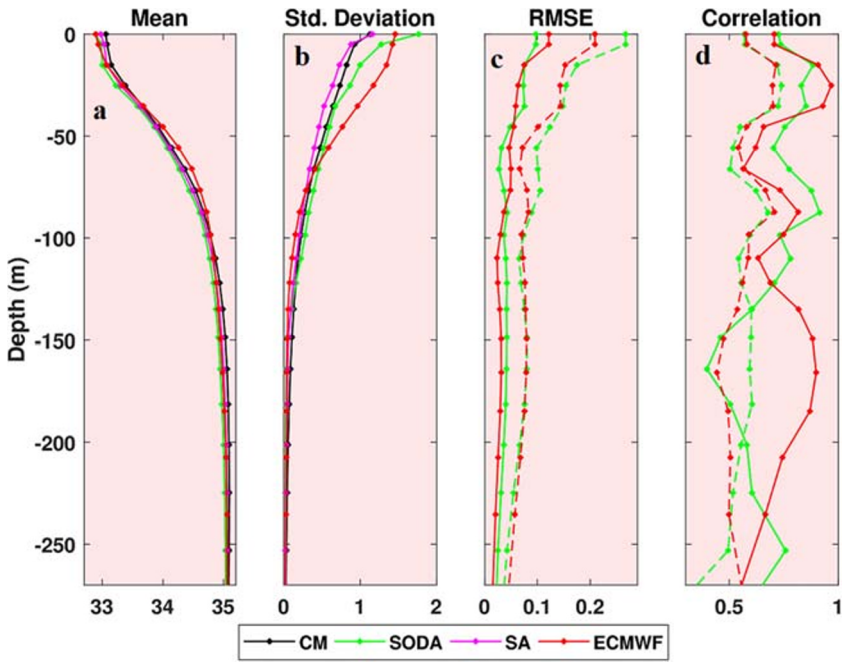

Fig. 8 Vertical profiles of salinity up to 270 m for the years 2010–2014 are compared for their mean and standard deviation with SODA and ECMWF. RMSE and Correlation are analysed between model results and each data. For RMSE and correlation, straight line shows with respect to coupled model while dotted line shows with respect to standalone model

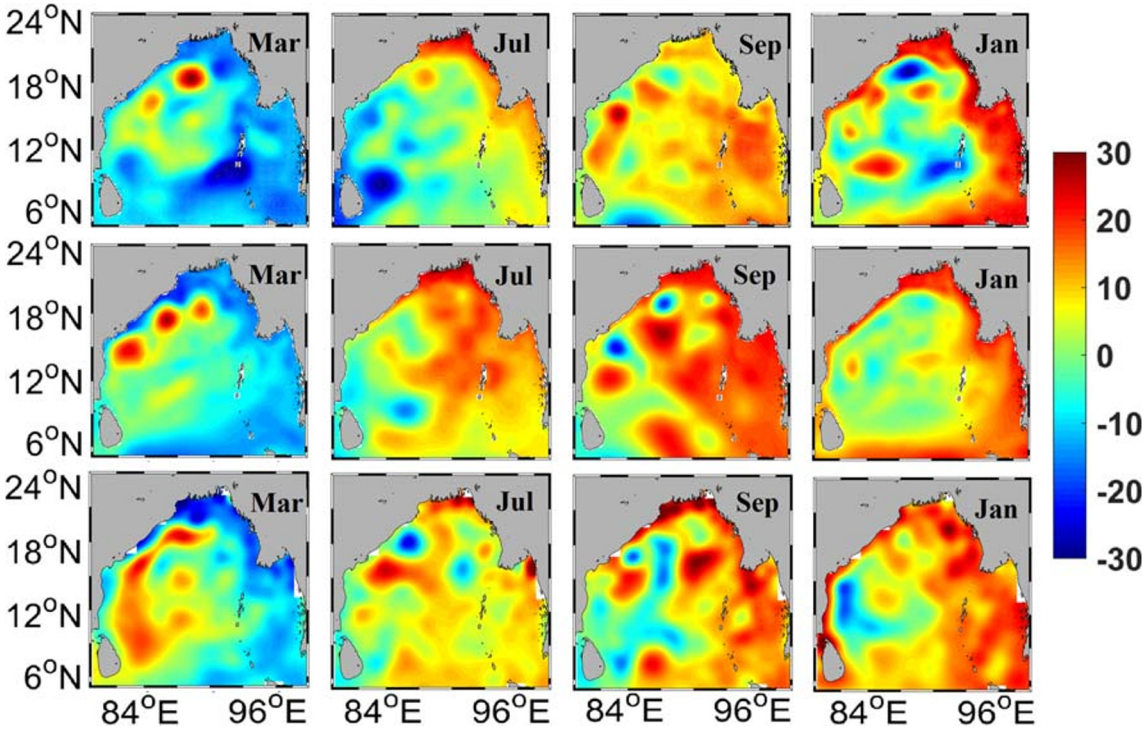

Fig. 9 Sea Level Anomaly (cm) for the months March, July, September and January of the year 2011 from (Top row) Standalone Model, (Middle row) Coupled model and (Bottom row) AVISO – TOPEX

downwelling Kelvin wave (2nd downwelling mode) is present throughout the bay along the coast in January, which is being well captured by the models. As the Kelvin waves are initiated and propagated due to remote equatorial forcings, this

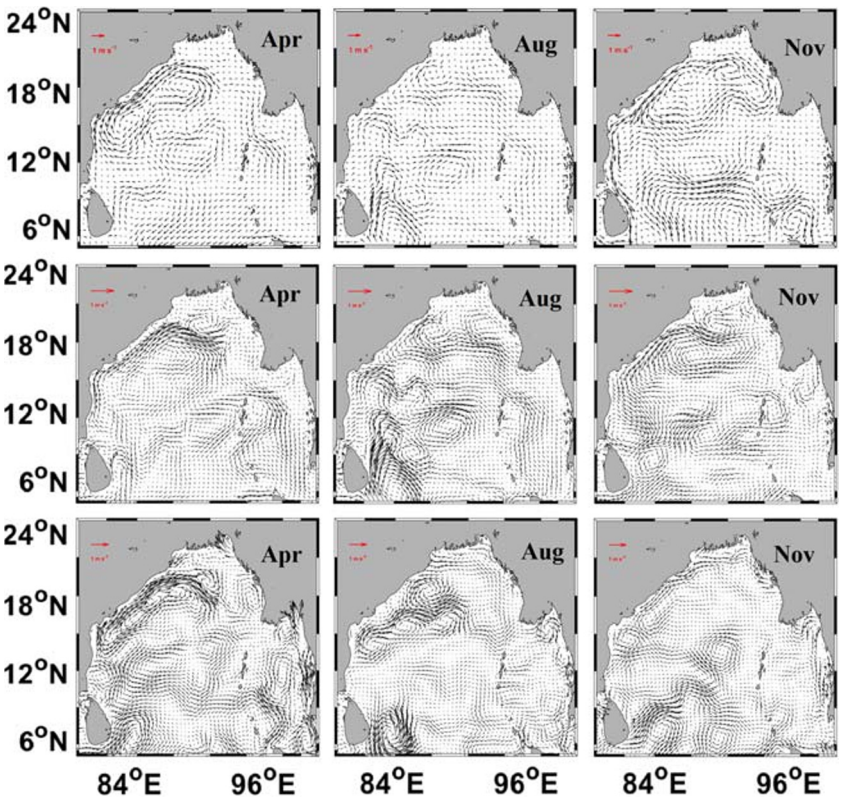

Fig. 10 Sea Surface Currents for the months April, August and November of the year 2011 from (Top row) Standalone Model, (Middle row) Coupled Model and (Bottom row) OSCAR surface velocities

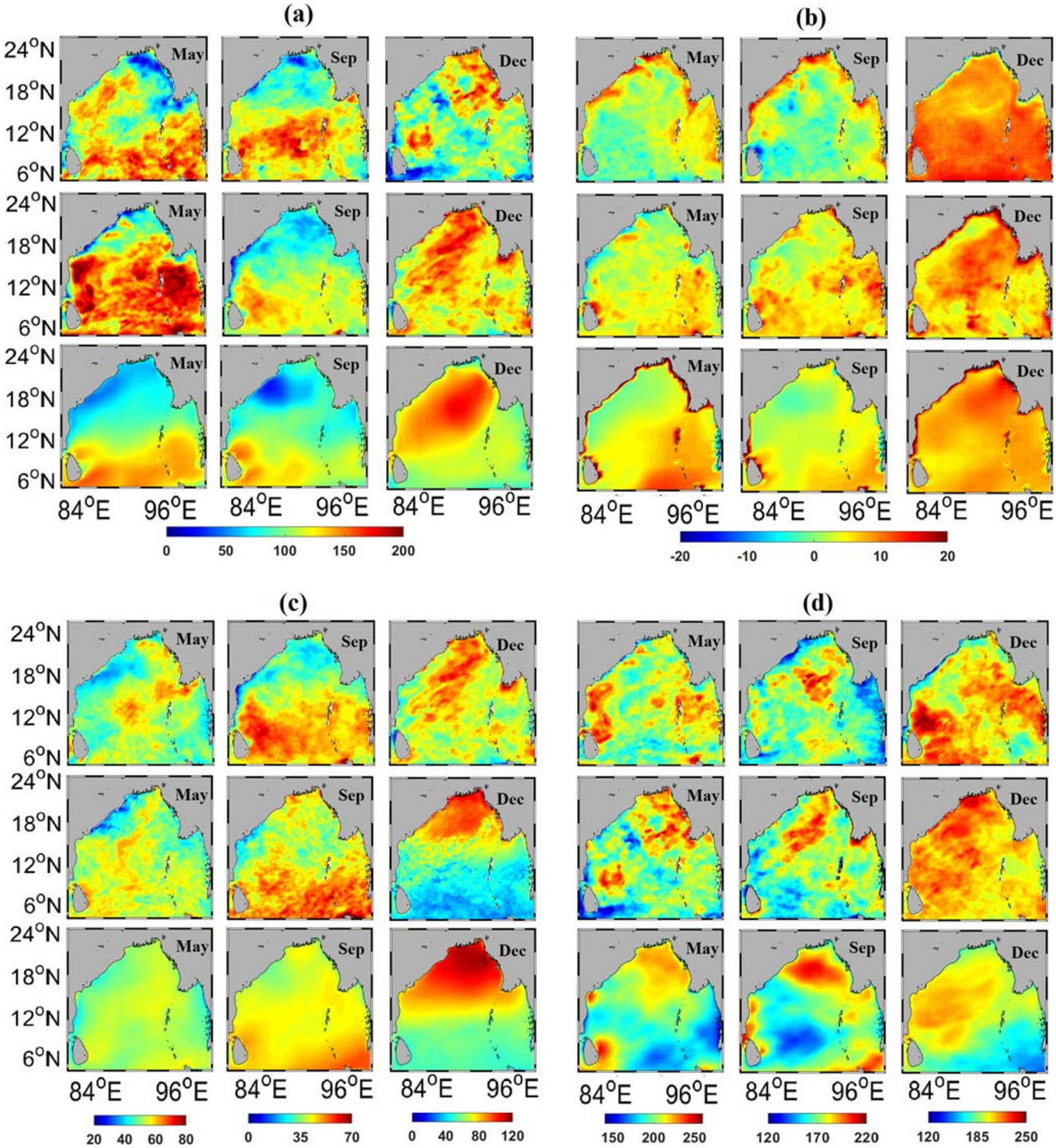

Fig. 11 Heat Flux analysis in Wm^{-2} for the months May, September and December of the year 2011 from (Top row) Standalone Model, (Middle row) Coupled Model and (Bottom row) MERRA reanalysis products for a. Latent heat flux b. Sensible heat flux c. Net outgoing longwave radiation d. Net downward Shortwave Radiation

evaluation indicate the ability of the coupled model to simulate the remote forcing signals with lateral boundary conditions. Also, the variation in the SSH along the coastal regions is reproduced well in comparison to satellite data. The upwelling and downwelling region in the western boundary currents are also captured very well.

3.4 Sea Surface Currents

The BOB region experiences a unique seasonally reversing surface circulation every year in the extent of pre–monsoon to post monsoon season. During pre–monsoon season, the western boundary current is northwards, in accordance with the winds

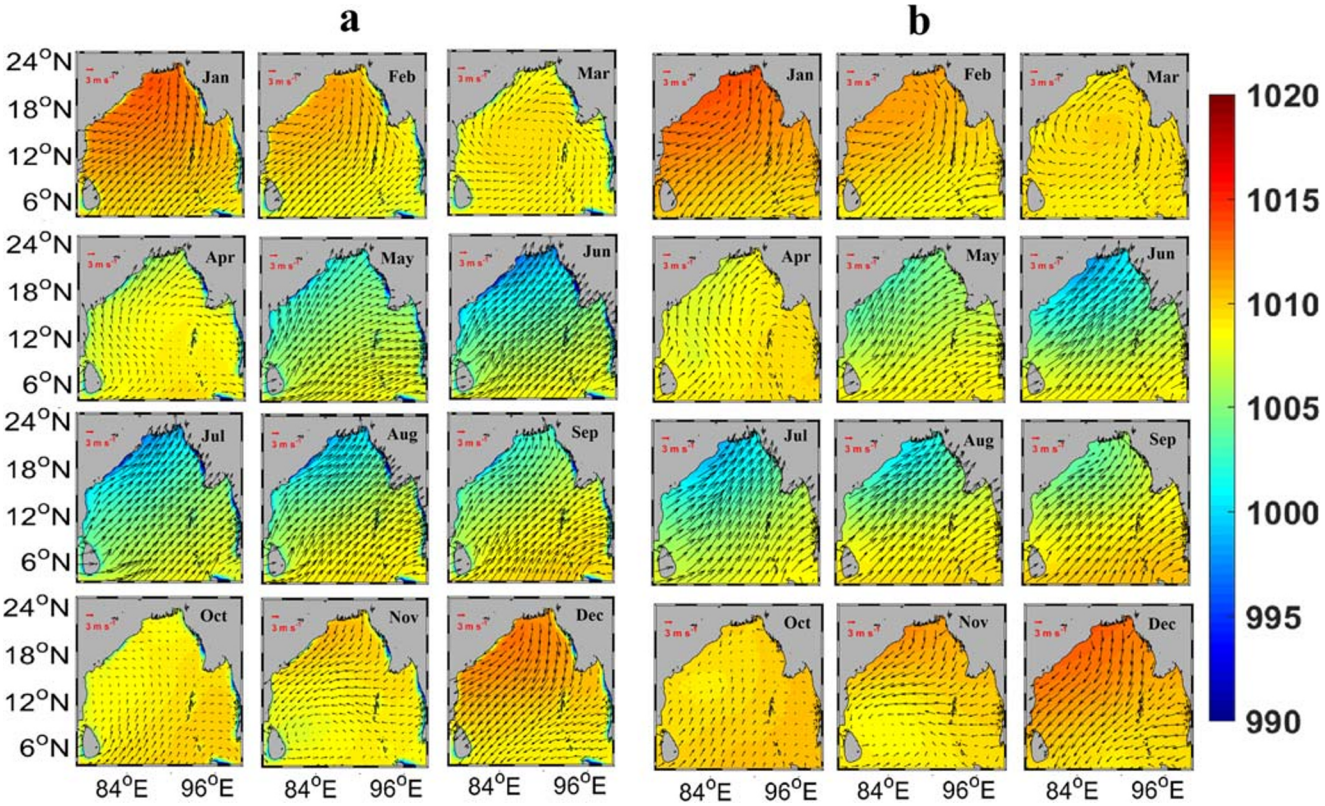

Fig. 12 Sea level Pressure (hPa) overlaid with 10 m wind speed (ms^{-1}) for the year 2011 from coupled model (**a**) and MERRA (**b**) sea level pressure and ASCAT surface winds

blowing over the bay in that period. Along the northern bay, first the reversal occurs during late monsoon season turning the flow southwards. This reversal causes the meeting of northward and southward currents along the north western bay and makes a discontinuous boundary current and a new zonal current towards eastward. This current is embedded with numerous eddies along both sides of the zonal current. With the arrival of northeast monsoon winds, the reversal completes and the boundary flow becomes entirely southwards during the post monsoon season. The three phases, northwards during pre–monsoon (April), discontinuous currents during monsoon (August) and southwards during post–monsoon season (November) are reproduced well by the models. The surface currents for the above mentioned months of the year 2011 are compared to OSCAR data in Fig. 10. The models are able to reproduce the surface circulation along the boundary currents and associated eddies very well. Along the southern boundary, near the Sri Lanka coast, the simulation shows the formation of cyclonic and anticyclonic eddies. The direction and magnitude of the currents are also well simulated by the model and are comparable with that of the OSCAR data.

3.5 Surface Heat Fluxes

Surface heat flux is an important parameter in the air–sea interactions occurring at the boundary layer of atmosphere. Here, in the Taylor diagram comparison in Fig. 2e, the coupled model calculated net surface heat flux has a correlation of 0.91 as compared to heat flux obtained from MERRA data. The RMSD between model and MERRA net heat flux is quite large (~35 Wm^{-2}) and the standard deviation is small. The standalone model also shows similar correlation as coupled model but the RMSD and standard deviation are higher than the coupled model. For individual analysis of the flux components, we compare the radiation and turbulent fluxes estimated by the models with MERRA data for the months of May, September and December for the year 2011. These months are selected because they have the maximum variation (Shenoi et al. 2002) between north and south bay, as well as among each month.

3.5.1 Turbulent Heat Fluxes

Latent heat flux at the sea surface indicates the energy exchange due to evaporation. The release of latent heat causes cooling on the upper ocean surface and increase in salinity because of evaporation. The model simulations capture these exchanges well and are compared with satellite data in Fig. 11. Here, the latent heat flux is maximum near the southern bay in May and September. In December, the northern bay shows the maximum latent heat flux. In May, the models record high sensible heat flux in the south–eastern bay as shown by the

MERRA data. In September, the southern bay registers high sensible heat flux as compared to the northern bay and it reverses in December. The coupled model results have lesser bias when compared to MERRA data than the standalone model.

3.5.2 Radiative Heat Fluxes

The net Outgoing Longwave Radiation (OLR) and the net Incoming Solar Radiation (ISR) flux are compared in Fig. 11c–d. The net OLR is better simulated by the coupled model. In the month of May and August, the OLR is fairly uniform over the bay ranging, from 50 to 60 Wm^{-2} but there is a distinct difference between southern and northern bay in December. The southern bay shows the OLR as 40–50 Wm^{-2} while the north shows as 110–120 Wm^{-2} in December. This change in OLR for different months is also in good agreement with that found in MERRA data. For the ISR, both the models simulate reasonably well to be compared with satellite data. The ISR is maximum along the northern bay where it ranges from 200 to 220 Wm^{-2}.

3.6 Sea Level Pressure, Surface Winds and Top of the Atmosphere

The atmospheric component of the coupled model is able to accurately simulate the Sea Level Pressure (SLP), Surface Winds (SW) at 10 m height, geopotential height at 500 mb and temperature at 200 mb pressure level. The model results for SLP and SW during the year 2011 are compared with MERRA sea level pressure satellite data and ASCAT surface winds in Fig. 12. The model simulates seasonal reversal of surface winds over the bay very well. The minute features of northeast monsoon winds are even present in January and February month results. During May, the southwest wind sets off along the east coast of India that generates an anti–cyclonic circulation over the bay. This circulation weakens and the southwest winds become stronger for the next six months. The winds are strongest in the month of June and are almost absent in October. The northeast monsoon winds set over the bay during the month of November and initiates the cycle again. The monthly SLP variations over the bay, splits the bay into two regions, the southeast and northwest. In the southeast bay, the SLP remains very high throughout the year, while the northwest bay shows a semi–annual pattern of SLP. During the summer monsoon period, the northwest bay shows low SLP while in the winter monsoon, it shows high values of SLP. This pattern of SLP and surface winds correlate well with the satellite data derived from MERRA and ASCAT. The Taylor diagram for SLP and SW in Fig. 2f and g shows that both SLP and SW are simulated by the model well with very high correlation (0.99 for SLP and 0.97 for SW) with the satellite data.

The model derived 500 mb geopotential height and 200 mb temperature are compared with NCEP– FNL and NCEP–CFS data in the Taylor diagrams Fig. 2h and i respectively. The simulated geopotential height at the 500 mb has a correlation of 0.98 with a mean standard deviation of 20 m with NCEP–CFS data. The temperature at 200 mb has a correlation of 0.97 with a mean standard deviation of 2 °C when compared to NCEP–CFS data. These high correlations and small standard deviation indicate the model is able to simulate the top of the atmosphere very well, including the interannual variability.

4 Conclusions

A regional coupled model with ROMS as oceanic component and WRF as atmospheric component is compared with standalone ocean model ROMS for their ability to reproduce the oceanic and atmospheric state over the Bay of Bengal. Both models simulate the surface and subsurface temperature with high accuracy compared to satellite and reanalysis data, however the interannual variability in SST is captured well by the coupled model (correlation coefficient is 0.96 compared to TRMM TMI). The simulations overestimate the surface salinity in the northern bay where the freshwater influx occurs. The evolution of surface salinity with the coupled model has a correlation of 0.78 and a bias of 0.25 psu when compared with SODA. The models simulate the Kelvin wave propagation along the bay that shows the capability of the models to capture the equatorial remote forcings. The surface currents simulated by both models reproduces the seasonal reversal of WBC as compared to the OSCAR data. The heat fluxes at the surface waters are evaluated with MERRA and other satellite products. Other than the little variations in shortwave radiations, the models are able to reproduce the satellite measurements. The evolution of net heat flux during the simulation period has a correlation of 0.91 as compared to MERRA data from the coupled model. The model simulations of sea level pressure and surface wind speed match well with satellite data as indicated by the good correlation (0.97 and 0.99) between them. The details of the top of the atmosphere are also better captured by the model. Even though the standalone model captures the oceanic parameters well, the near surface parameters from ocean and atmosphere, and their interactions are better replicated by coupled model. Therefore, the study suggests that the couple model is useful for the regional studies on ocean and atmospheric processes.

Acknowledgements The data used in this effort were acquired as part of the activities of NASA's Science Mission Directorate, and are archived and distributed by the Goddard Earth Sciences (GES) Data and Information Services center (DISC). We further acknowledge Indian Institute of Technology Kharagpur, Ministry of Human Resources and Development, Ministry of Earth Sciences, University Grants Commission and DST Climate Change SPLICE MDRP of The Government of India

for providing facility and funds for this study. JK acknowledges the SRIC/CMI project of IIT Kharagpur for additional funding. Data used in the analysis (SODA from http://www.atmos.umd.edu/~ocean/index_files/soda3.3.1_mn_download.htm, ECMWF–ORAS4 from https://www.ecmwf.int/en/research/climate-reanalysis/ocean-reanalysis, NCEP–GODAS from http://www.cpc.ncep.noaa.gov/products/GODAS/, NCEP–FNL from https://rda.ucar.edu/datasets/ds083.2/, NCEP–CFS from https://rda.ucar.edu/datasets/ds094.2/, World Ocean Database from https://www.nodc.noaa.gov/OC5/SELECT/dbsearch/dbsearch.html, TRMM TMI from http://www.remss.com/missions/tmi/#data_access, AVISO TOPEX from http://apdrc.soest.hawaii.edu/dods/public_data/satellite_product/TOPEX/VISO_upd/ msla_monthly_clima, OSCAR from http://podaac.jpl.nasa.gov/dataset/OSCAR_L4_OC_ third-deg, MERRA from https://gmao.gsfc.nasa.gov/reanalysis/MERRA-2/, ASCAT available at http://apdrc.soest.hawaii.edu/datadoc/ascat.php, ARGO through the IPRC Argo Dataset (available at http://apdrc.soest.hawaii.edu/projects/argo/), RAMA buoy data NOAA website (https://www.pmel.noaa.gov/tao/drupal/disdel/) are greatly acknowledged.

References

Babu, M. T.: Equatorward western boundary current in the Bay of Bengal during November–December 1983. Physical Processes in the Indian Seas (Proceedings of First Convention, ISPSO), pp. 57–62.(1992)

Balmaseda, M.A., Mogensen, K., Weaver, A.T.: Evaluation of the ECMWF ocean reanalysis system ORAS4. Q.J.R. Meteorol. Soc. **139**, 1132–1161 (2013). https://doi.org/10.1002/qj.2063

Bentamy, A., Fillon, D.C.: Gridded surface wind fields from Metop/ASCAT measurements. Int. J. Remote Sens. **33**(6), 1729–1754 (2012). https://doi.org/10.1080/01431161.2011.600348

Bonjean, F., Lagerloef, G.S.E.: Diagnostic model and analysis of the surface currents in the tropical Pacific Ocean. J. Phys. Oceanogr. **32**, 2938–2954 (2002). https://doi.org/10.1175/1520-0485(2002)032%3C2938:DMAAOT%3E2.0.CO;2

Boyer, T. P., Antonov, J. I., Baranova, O. K., Coleman, C., Garcia, H. E., Grodsky, A., Johnson, D. R. Locarnini, R. A., Mishonov, A. V., O'Brien, T. D., Paver, C. R., Reagan, J. R., Seidov, D., Smolyar, I. V. and Zweng, M. M.: World Ocean Database 2013. Silver Spring, MD, NOAA Printing Officce, 208pp. (NOAA Atlas NESDIS, 72) (2013) https://doi.org/10.7289/V5NZ85MT

Carton, J.A., Chepurin, G.A., Chen, L.: SODA3: a new ocean climate reanalysis. J. Clim. **31**(17), 6967–6983 (2018)

Chakraborty, A., Gangopadhyay, A.: Development of a high-resolution multiscale modeling and prediction system for bay of Bengal. Part I: Climatology-Based Simulations. O. J. Mar. Sci. **6**, 145–176 (2016a). https://doi.org/10.4236/ojms.2016.61013

Chakraborty, A., Gangopadhyay, A.: Development of a high-resolution multiscale modeling and prediction system for bay of Bengal, part II: an application to October 2008. O. J. Mar. Sci. **6**, 125–144 (2016b). https://doi.org/10.4236/ojms.2016.61012

Cutler, A. N., and Swallow, J. C.: Surface currents of the Indian Ocean (to 25 S to 100 E), Report No. 87. Institute of Oceanographic Sciences, Broadchill, UK. (1984)

da Silva, A. M., Young, C. C., Levitus, S.: Atlas of Surface Marine Data 1994 Volume 1: Algorithms and Procedures, NOAA Atlas NESDIS 6, US Dept.Commerce, Washington DC. (1994)

Dandapat, S., Chakraborty, A.: Mesoscale eddies in the Western Bay of Bengal as observed from satellite altimetry in 1993–2014: statistical characteristics, variability and three dimensional properties. IEEE J. Sel. Topics Appl. Earth Observ. Remote Sens. **9**(11), 5044–5054 (2016). https://doi.org/10.1109/JSTARS.2016.2585179

Das, B.K., Anandh, T.S., Kuttippurath, J., Chakraborty, A.: Characteristics of the Discontinuity of Western Boundary Current in the Bay of Bengal. J. Geophys. Res.: Oceans. **124**, 4464–4479 (2019). https://doi.org/10.1029/2019JC015235

Dee, D.P., Uppala, S.M., Simmons, A.J., Berrisford, P., Poli, P., Kobayashi, S., Andrae, U., Balmaseda, M.A., Balsamo, G., Bauer, D.P., Bechtold, P.: The ERA-interim reanalysis: configuration and performance of the data assimilation system. Q. J. R. Meteorol. Soc. **137**(656), 553–597 (2011). https://doi.org/10.1002/qj.828

Ducet, N., Le Traon, P.Y., Reverdin, G.: Global high-resolution mapping of ocean circulation from TOPEX/Poseidon and ERS-1 and -2. J. Geophys. Res. **105**(C8), 19477–19498 (2000). https://doi.org/10.1029/2000JC900063

Elsberry, R.L., Garwood Jr., R.W.: Sea-surface temperature anomaly generation in relation to atmospheric storms. Bull. Am. Meteorol. Soc. **59**(7), 786–789 (1978)

Fairall, C.W., Bradley, E.F., Hare, J.E., Grachev, A.A., Edson, J.B.: Bulk parameterization of air–sea fluxes: updates and verification for the COARE algorithm. J. Clim. **16**(4), 571–591 (2003). https://doi.org/10.1175/1520-0442(2003)016<0571:BPOASF>2.0.CO;2

Girishkumar, M.S., Ravichandran, M.: The influences of ENSO on tropical cyclone activity in the bay of Bengal during October–December. J. Geophys. Res. **117**, C02033 (2012). https://doi.org/10.1029/2011JC007417

Goswami, B.N., Krishnamurthy, V., Annmalai, H.: A broad-scale circulation index for the interannual variability of the Indian summer monsoon. Q. J. R. Meteorol. Soc. **125**(554), 611–633 (1999)

Haidvogel, D.B., Arango, H., Budgell, W.P., Cornuelle, B.D., Curchitser, E., Di Lorenzo, E., Fennel, K., Geyer, W.R., Hermann, A.J., Lanerolle, L., Levin, J.: Ocean forecasting in terrain-following coordinates: formulation and skill assessment of the Regional Ocean modeling system. J. Comput. Phys. **227**(7), 3595–3624 (2008). https://doi.org/10.1016/j.jcp.2007.06.016

Jana, S., Gangopadhyay, A., Chakraborty, A.: Impact of seasonal river input on the bay of Bengal simulation. Cont. Shelf Res. **104**, 45–62 (2015). https://doi.org/10.1016/j.csr.2015.05.001

Kalnay, E., Kanamitsu, M., Kistler, R., Collins, W., Deaven, D., Gandin, L., Iredell, M., Saha, S., White, G., Woollen, J., Zhu, Y.: The NCEP/NCAR 40-year reanalysis project. Bull. Am. Meteorol. Soc. **77**(3), 437–471 (1996). https://doi.org/10.1175/1520-0477(1996)077%3C0437:TNYRP%3E2.0.CO;2

Kumar, B., Sil, S., Pandey, P.C., Chakraborty, A.: Seasonal and monthly variation of vertical structure of temperature, salinity and heat flux of the bay of Bengal. Mar. Geod. **33**(1), 76–99 (2010)

Lebedev, K.V., DeCarlo, S., Hacker, P.W., Maximenko, N.A., Potemra, J.T., Shen, Y.: Argo products at the asia-pacific data-research center. Eos. Transactions American Geophysical Union. **91**(26), (2010)

Legeckis, R.: Satellite observations of a western boundary current in the bay of Bengal. J. Geophys. Res. **92**(C12), 12974–12978 (1987). https://doi.org/10.1029/JC092iC12p12974

McPhaden, M.J., Meyers, G., Ando, K., Masumoto, Y., Murty, V.S.N., Ravichandran, M., Syamsudin, F., Vialard, J., Yu, L.'., Yu, W.: RAMA: The Research Moored Array for African-Asian-Australian Monsoon Analysis and Prediction. Bull. Am. Meteorol. Soc. **90**, 459–480 (2009)

Menemenlis, D., Fukumori, I., Lee, T.: Using Green's functions to calibrate an ocean general circulation model. Mon. Weather Rev. **133**(5), 1224–1240 (2005). https://doi.org/10.1175/MWR2912.1

Menemenlis, D., Campin, J.M., Heimbach, P., Hill, C., Lee, T., Nguyen, A., Schodlok, M., Zhang, H.: ECCO2: high resolution global ocean and sea ice data synthesis. Mercator Ocean Quarterly Newsletter. **31**(October), 13–21 (2008)

Prasad, T.G.: Annual and seasonal mean buoyancy fluxes for the tropical Indian Ocean. Current Science. 667–674 (1997)

Rienecker, M.M., Suarez, M.J., Gelaro, R., Todling, R., Bacmeister, J., Liu, E., Bosilovich, M.G., Schubert, S.D., Takacs, L., Kim, G.K., Bloom, S.: MERRA: NASA's modern-era retrospective analysis for research and applications. J. Clim. **24**(14), 3624–3648 (2011). https://doi.org/10.1175/JCLI-D-11-00015.1

Saha, S., Moorthi, S., Wu, X., Wang, J., Nadiga, S., Tripp, P., Behringer, D., Hou, Y., Chuang, H., Iredell, M., Ek, M., Meng, J., Yang, R., Mendez, M. P., van den Dool, H., Zhang, Q., Wang, W., Chen, M., and Becker, E.: NCEP Climate Forecast System Version 2 (CFSv2) Monthly Products. Research Data Archive at the National Center for Atmospheric Research, Computational and Information Systems Laboratory. Dataset. (2012) https://doi.org/10.5065/D69021ZF. Accessed 29 nov 2017

Shchepetkin, A.F., McWilliams, J.C.: The regional oceanic modeling system (ROMS): a split-explicit, free-surface, topography-following-coordinate oceanic model. Ocean Model. **9**(4), 347–404 (2005). https://doi.org/10.1016/j.ocemod.2004.08.002

Shenoi, S.S.C., Shankar, D., Shetye, S.R.: Differences in heat budgets of the near-surface Arabian Sea and Bay of Bengal: Implications for the summer monsoon. Journal of Geophysical Research: Oceans. **107**(C6), (2002). https://doi.org/10.1029/2000JC000679

Shetye, S.R., Gouveia, A.D., Shenoi, S.S.C., Sundar, D., Michael, G.S., Almeida, A.M., Santanam, K.: Hydrography and circulation off the west coast of India during the southwest monsoon 1987. J. of Mar. Res. **48**(2), 359–378 (1990). https://doi.org/10.1357/002224090784988809

Sil, S., Chakraborty, A.: Simulation of East India coastal features and validation with satellite altimetry and drifter climatology. Int. J. of Oce. and Clim. Sys. **2**(4), 279–289 (2011a)

Sil, S., Chakraborty, A.: Numerical simulation of seasonal variations in circulations of the bay of Bengal. Journal of Oceanography and Marine Science. **2**(5), 127–135 (2011b)

Sil, S., Chakraborty, A. and Ravichandran, M.: Numerical simulation of surface circulation features over the bay of bengal using regional ocean modeling system. In Advances in Geosciences: Volume 24: Ocean Science (OS) (pp. 117–130). (2011)

Sivareddy, S., Ravichandran, M., Girishkumar, M.S., Prasad, K.V.S.R.: Assessing the impact of various wind forcing on INCOIS-GODAS simulated ocean currents in the equatorial Indian Ocean. Ocean Dyn. **65**(9–10), 1235–1247 (2015). https://doi.org/10.1007/s10236-015-0870-6

Skamarock, W. C., Klemp, J. B., Dudhia, J., Gill, D. O., Barker, D. M., Wang, W. and Powers, J.G.: A description of the Advanced Research WRF version 3. NCAR Technical note-475+ STR. 113 pp. (2008) doi:https://doi.org/10.5065/D68S4MVH

Srivastava, A., Dwivedi, S., Mishra, A.K.: Intercomparison of high-resolution bay of Bengal circulation models forced with different winds. Mar. Geod. **39**(3–4), 271–289 (2016). https://doi.org/10.1080/01490419.2016.1173606

Subramanian, V.: Sediment load of Indian rivers. Current Science. 928–930 (1993)

Suryanarayana, A., Murty, V.S.N., Sarma, Y.V.B., Babu, M.T., Rao, D.P., Sastry, J.S.: In: Desai, B.N. (ed.) Hydrographic features of the western Bay of Bengal in the upper 500 m under the influence of NE and SW monsoon, pp. 595–604. Oxford and IBH Publishing, New Delhi (1992) http://drs.nio.org/drs/handle/2264/3101

Taylor, K.E.: Summarizing multiple aspects of model performance in a single diagram. Journal of Geophysical Research: Atmospheres. **106**(D7), 7183–7192 (2001)

Trenberth, K.E.: The definition of el nino. Bull. Am. Meteorol. Soc. **78**(12), 2771–2777 (1997)

Vinayachandran, P.N., Shetye, S.R.: The warm pool in the Indian Ocean. Proceedings of the Indian Academy of Sciences-Earth and Planetary Sciences. **100**(2), 165–175 (1991). https://doi.org/10.1007/BF02839431

Warner, J.C., Armstrong, B., He, R., Zambon, J.B.: Development of a coupled ocean–atmosphere–wave–sediment transport (COAWST) modeling system. Ocean Model. **35**(3), 230–244 (2010). https://doi.org/10.1016/j.ocemod.2010.07.010

Wentz, F. J., Gentemann, C. and Hilburn, K. A.: Remote Sensing Systems TRMM TMI [Monthly] Environmental Suite on 0.25 deg grid, Version 7.1, Remote Sensing Systems, Santa Rosa, CA. Available online at www.remss.com/missions/tmi. (2015) [Accessed 25 Oct 2017]